Bridge Aerodynamics, Larsen & Esdahl (eds) © 1998 Balkema, Rotterdam, ISBN 90 5410 961 0

Uncertainties of extreme winds, spectra, and coherences

J. Mann, L. Kristensen & N.O. Jensen
Risø National Laboratory, Roskilde, Denmark

ABSTRACT: The uncertainty on the the 50-year storm can be estimated from two widely used methods: the peak over threshold and the maximum model. Long records of wind speeds are usually but not always in agreement with the basic model assumptions. At moderate to high frequencies there is a good agreement among researchers on spectral shapes over homogeneous terrain assuming neutral atmospheric stability. Neutral stability at high wind speeds is a rule with exceptions and despite of high wind speeds an example from the Great Belt Coherence Experiment shows greatly reduced turbulence levels. At low frequencies there is still some discrepancies among model spectra. Due to modeling work based on the Great Belt Coherence Experiment the coherences are well predicted once the spectra are known. Strong wind turbulence in inhomogeneous terrain, which is often the setting of bridges, is an area of active research.

1 INTRODUCTION

Estimating loads on structures requires an estimate of the most probable worst storm over expected life time of the structure, together with spectra and coherences of the gusty wind. Probabilistic design methods in engineering require an estimate of the uncertainties of the, say, 50-years storm, the design spectra and coherences. In this paper the uncertainties of each of these are reviewed.

2 EXTREME WINDS

There are two widely used methods to estimate the return period of a given wind speed (or equivalently the n-years storm) given a record of measured wind speeds. The record consists typically of 10 minutes averages.

The concept of extreme winds can also be applied to gusts. Kristensen et al. (1991) give a systematic definition of gusts, but we shall only treat the extreme of the 10 minutes mean wind in this section.

2.1 *Peak over threshold (POT)*

POT consists of collecting all storms greater than a given threshold U' (see Figure 1). These are assumed to occur in a random and stationary manner like a Poisson process with an average rate λ and have an exponential probability distribution of wind speeds. Thus by assumption the cumulative distribution of peak exceedances over U' has the form

$$F(U) = 1 - \exp\left(-\frac{U - U'}{\alpha}\right) \quad \text{for } U > U', \qquad (1)$$

where α is the mean of the exceedance. The probability of a wind speed being *larger* than U is therefore $\exp(-(U - U')/\alpha)$. Since we have assumed the storms (or peak exceedances) to occur randomly in time the average number of storms with wind speeds higher than the threshold U' in a period of length T is

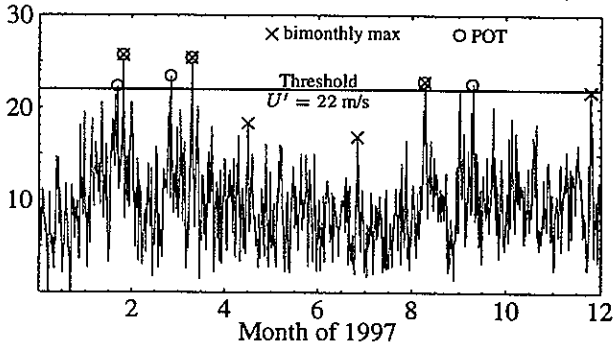

Figure 1: The difference between POT and periodical maximum illustrated by data from the Great Belt 70 meter mast in 1997.

λT, and the average number of storms stronger than some higher level U is $\lambda_T = \lambda T \exp(-(U - U')/\alpha)$. The definition of the T-year storm U_T (if T is measured in years) is the highest wind speed than on average will occur once in the period T, thus we have to solve the equation $\lambda_T = 1$

$$U_T = U' + \alpha \ln(\lambda T), \tag{2}$$

showing the dependence of the T-year storm U_T on T.

Suppose we have data for the period T_{data} and the number of storms in this period is N then the the parameters can be estimated as (Abild 1994)

$$\lambda \approx \frac{N}{T_{\text{data}}}, \quad \alpha \approx \overline{U} - U', \tag{3}$$

which are the so-called maximum likelihood estimates. It is clear that the uncertainties on these estimates will affect the uncertainty of the T-year estimate (2). Using properties of the exponential distribution and the Poisson process, and using the propagation of variance formula, we can estimate the uncertainty of U_T from (2). The result is

$$\sigma(U_T) \approx \frac{\alpha}{\sqrt{\lambda T_{\text{data}}}} \sqrt{1 + \ln^2(\lambda T)} \tag{4}$$

(Abild 1994), which shows that the longer the period of data collection T_{data} the smaller the error.

2.2 *Periodical maximum method*

The periodical maximum method, which is probably the most widely used, consists dividing the record of wind speeds into n periods of equal length, typically one year or less. Then, a new record of extreme winds $U_1^{\max}, \ldots, U_n^{\max}$ is constructed by taking the maximum of each period and sorting them in ascending order. It can be shown, that if the tail of the distribution of winds is exponential then the extreme winds have (asymptotically) an accumulated probability which is double exponential (Gumbel 1958)

$$F(U) = \exp\left(-\exp[-\alpha(U - \beta)]\right). \tag{5}$$

A fairly simple method to extract the parameters from (5) which, according to Abild (1994), has proven highly efficient for even small size samples is the following. First

$$b_1 = \frac{1}{n} \sum_{i=1}^{n} \frac{i-1}{n-1} U_i^{\max} \tag{6}$$

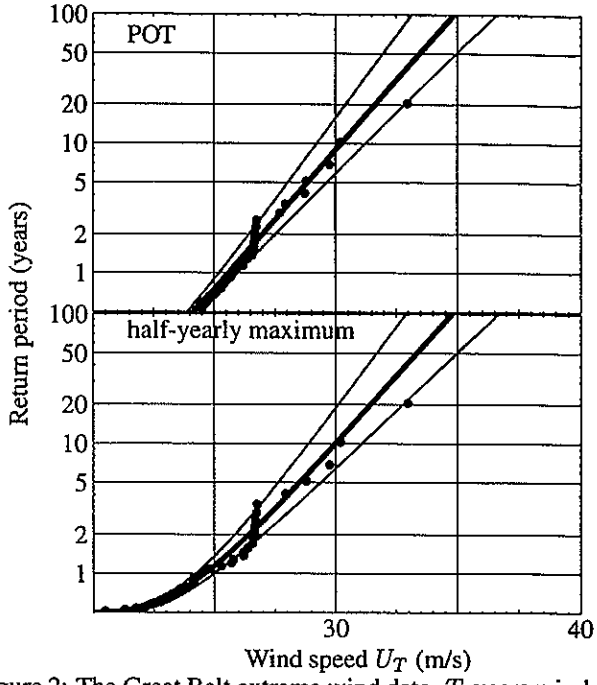

Figure 2: The Great Belt extreme wind data. T-years wind speed as a function of return period. The one σ error on the T-year storm is indicated by thin lines. See the text.

is calculated, and then the parameters are estimated as

$$\alpha = \frac{\ln 2}{2b_1 - \overline{U^{\max}}}, \quad \beta = \overline{U^{\max}} - \frac{\gamma}{\alpha}, \tag{7}$$

where γ is Euler's constant ≈ 0.577216, and $\overline{U^{\max}}$ the mean of the maximum values.

Once the parameters α and β are found the T-year wind speed U_T can be found from the following equation relating the recurrence interval T to the cumulative probability

$$T = \frac{1}{1 - F(U_T)}. \tag{8}$$

Solving this equation we get

$$U_T = -\alpha^{-1} \ln \ln \frac{T}{T-1} + \beta. \tag{9}$$

Again the uncertainty of U_T can be calculated from the uncertainties on α and β. Lengthy calculations give

$$\sigma(U_T) = \frac{\pi}{\alpha} \sqrt{\frac{1 + 1.14 k_T + 1.10 k_T^2}{6n}} \tag{10}$$

where

$$k_T = -\frac{\sqrt{6}}{\pi} \left[\ln \ln \left(\frac{T}{T-1} \right) - \gamma \right]. \tag{11}$$

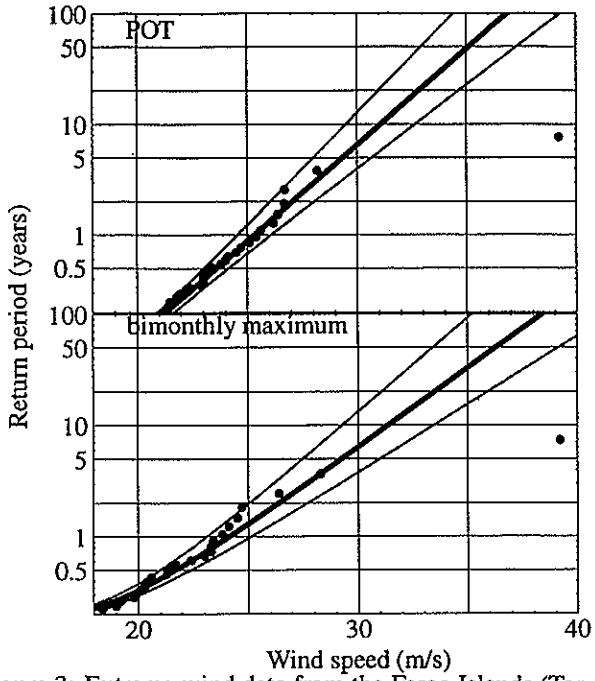

Figure 3: Extreme wind data from the Faroe Islands (Torshavn). See caption of Figure 2.

This method is not terribly different from fitting a straight line to $U_i^{\max}$ versus $-\ln(-ln\frac{i}{n+1})$[1] and estimating the uncertainty of an extrapolations along this line. However, according to Abild (1994), the described method should be close to optimal with regards to bias and variance of the parameter estimates.

2.3 *Examples*

To illustrate the two methods two records will be analysed. The first is a 20 year long time series from the small island of Sprogø in the middle of the Great Belt. The measurements were made by a cup anemometer at 70 m above sea level, which corresponds to the height of the Great Belt East Bridge. A description of the meteorological station is given in Jensen, Nielsen, and Nielsen (1988).

The other is a bit over seven years long record from the Faroe Islands where Risø National Laboratory in the fall of 1987 installed a number of meteorological stations. The purpose was primarily to study the wind conditions at a range of typical topographic sites. The study is done on behalf of the local authority. Already before the end of the second year we had on record what still in 1998, after more than 10 years of operation, seems to be an outstanding storm. The 39.2 m/s (10 min. average) was measured at the station Glyvursnaes, which is considered not to be influenced by the local topography. At a station situated in a saddle point some kilometers away, 267 m a.s.l., called Nordredalsskard, the largest 10 min. mean speed was 58.1 m/s. About an hour later when the wind had turned so that the station came in the wake of the peak to the one side of the pass the mean wind decreased but the turbulent gusts (the largest 2 sec. mean value in each 10 min. period) increased to 76.7 m/s, at which point the lattice tower carrying the instrumentation collapsed and the recording stopped. This storm of 21-22 December 1988 is described in Petersen and Jensen (1995).

In Figure 2 the T-year storm U_T versus return period T according to (8) is shown both as derived from the data (dots) and as obtained from the equations (2) for POT and (9) for periodical maximum method (black broad lines). The $\pm\sigma$ lines from (4) and (10) are also shown. The Great Belt case, which is representative of the vast majority of extreme wind records, seems to comply with the assumptions underlying the two methods, and there seems not to be any significant difference between the two methods.

In Figure 3 the exceptional case of Faroe Islands is shown. When the monthly extremes are ordered we see that they order in a nice fashion except for the 39.2 m/s event which is completely off. The interpretation is that this particular event is of a different emsemble than the rest, i.e. pertaining to another phenomenon or include additional local effects such as a lee-wave phenomenon in the manner of the Chinook in the Boulder, Colorado area (Klemp and Lilly 1975). We obtain an average return period of approximately 300 years if this event is included. The problem is of course that if the so far singular event belongs to a different phenomenon than the rest of the extreme-value ensemble, the prediction value of the latter becomes irrelevant and the return period of the large storm could be a lot less than 300 years.

The uncertainties of the 50-year storm are shown in Table 1.

It should be noted that there has been done no correction for tower shadow effects, which can change the extreme wind estimates with a few m/s.

2.4 *Comparison*

The POT method has the advantage that it is very transparent. None of the methods gives a physical reason for exponential behaviour of the probability density functions. The POT method gives marginally smaller standard errors on the 50-year storm estimate. For the POT method the threshold U' has to be cho-

[1] That this is a straight line follows from the assumption (5).

Table 1: 50-years storms and their uncertainty by two methods and at two locations.

	Great Belt		Torshavn	
	POT	per. max	POT	per. max
record length	20 yrs		7.2 yrs	
# of storms	40	40	44	43
U' [m/s]	24.2	—	20.9	—
U_{50} [m/s]	33.5	33.3	35.1	36.3
$\sigma(U_{50})$ [m/s]	1.5	1.6	2.2	2.9

sen and likewise for the length of the n periods the periodical maximum. This introduces some arbitrariness into both methods. An additional choice has to be made for the POT method. In order to get independent storms all local maxima in an interval of, say, ± 1 day around a storm event do not count as independent storms. Usually, the predicted 50-year storm is not sensitive to these choices.

In conclusion, although the underlying assumptions are not exactly the same and the selected storms are not necessarily the same (see Figure 1) the methods give very similar results.

2.5 *Advances in determination of extreme winds*

In the analysis of extreme wind above there was no attempt to correct for local features of the landscape such as hills, varying roughness, and obstacles. In order to make long records of winds useful for extreme wind estimation at other location it is necessary to 'clean' the measured wind speeds of influences of the local terrain (Abild et al. 1992; Abild 1994). First, the wind speeds are corrected for varying roughnesses, hills and shelters. This gives a wind speed which would have been present if the surrounding terrain of the measuring mast were flat, with constant roughness and with no obstacles. The corrected wind speed is then extrapolated up to the top of the boundary layer giving the geostrophic (or 'free') wind speed. This is done via the geostrophic drag law which links the geostrophic wind to parameters describing the flow close to the surface (friction velocity and surface roughness).

Assuming that the geostrophic wind does not vary much with geographic location the whole procedure can be reversed to give extreme wind speeds at a different location with a different surface roughness distribution and topography.

The success of this procedure, called the wind atlas method (Mortensen et al. 1993), is based on the assumption that the geostrophic wind does not change from the measuring site to the site the extreme wind is going to be estimated. However, even over a relatively small area like Denmark there is a suspicion that the geostrophic wind is stronger over the western part than elsewhere in the country.

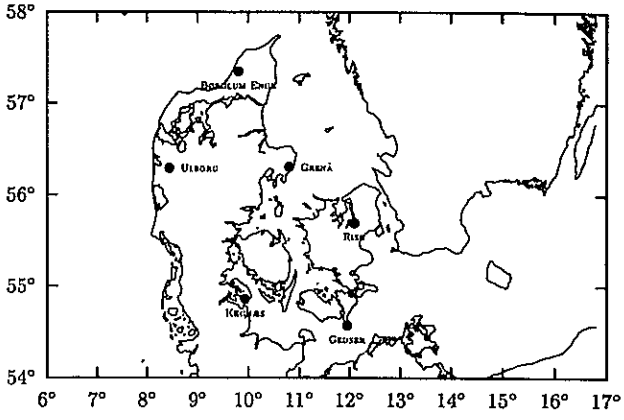

Figure 4: High precision pressure stations in Denmark installed early 1998.

To test this Risø has set up a net in Denmark of high precision sensors which are capable of measuring pressure within ± 0.25 hPa (see Figure 4). This will make it possible to measure horizontal pressure gradients with very high precision. The geostrophic wind is proportional to the magnitude of this gradient and its direction is perpendicular to it. The six stations in Figure 4 should be sufficient to detect variation in the extreme or mean geostrophic wind over Denmark.

3 SPECTRA AND COHERENCES

Since the vertical wind fluctuation w and the fluctuation in the mean wind direction u are of interest for bridge aerodynamics, we shall focus on these and not discuss transversal fluctuations v.

3.1 *Code and textbook spectra and coherences*

Surface layer scaling is used in many spectral models, implying that length scales are proportional to z and that variances are proportional to the square of the so-called friction velocity u_*^2 and not dependent on height. Defining a non-dimensional frequency $n \equiv fz/U$ the spectra[2] of Kaimal are (Kaimal et al. 1972; Kaimal and Finnigan 1995)

$$\frac{fS_u(f)}{u_*^2} = \frac{k_1 F_u(k_1)}{u_*^2} = \frac{52.5n}{(1+33n)^{5/3}}, \qquad (12)$$

[2]All spectra in this paper are 'two-sided' implying $\int_{infty}^{\infty} F(k_1)\mathrm{d}k_1 = \int_{-\infty}^{\infty} S(f)\mathrm{d}f$ is equal to the variance. The so-called 'one-sided' spectra, where $\int_0^{\infty} S(f)\mathrm{d}f$ is equal to the variance, are probably more commonly used.

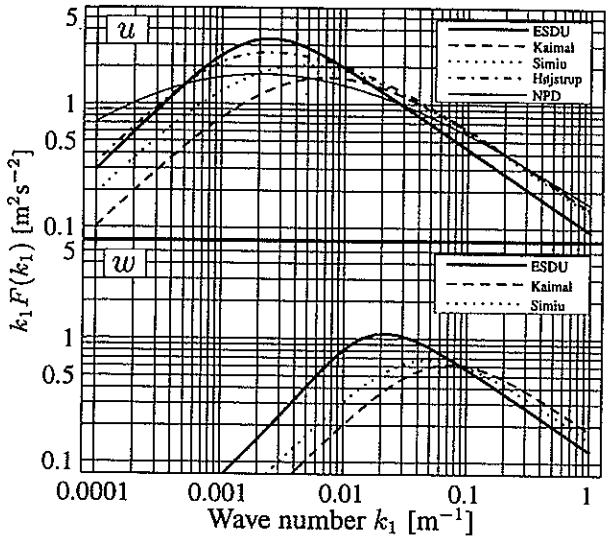

Figure 5: Comparison of spectral models as functions of $k_1 \equiv 2\pi f/U$. For the comparison $z = 40$ m and $U = 40$ m/s (over the sea) is chosen. For u ESDU, Kaimal (12), Simiu & Scanlan (14), Højstrup et al. (1990), and Norwegian Petroleum Directorate (1994) is used, and for w ESDU, Kaimal (13) and Simiu & Scanlan (15). A friction velocity of $u_* = 1.78$ m/s is used.

and

$$\frac{fS_w(f)}{u_*^2} = \frac{1.05n}{1 + 5.3n^{5/3}}. \tag{13}$$

Kaimal' s spectra are based on measurements over flat homogeneous terrain in Kansas.

The spectra of Simiu and Scanlan (1986) have the same functional shapes as Kaimal's but the numerical constants are different:

$$\frac{fS_u(f)}{u_*^2} = \frac{100n}{(1 + 50n)^{5/3}}, \tag{14}$$

and

$$\frac{fS_w(f)}{u_*^2} = \frac{1.68n}{1 + 10n^{5/3}}. \tag{15}$$

Deviations from surface layer scaling are found in the model spectra from ESDU International (1985). Also the spectra of Norwegian Petroleum Directorate (NPD 1994) and Højstrup et al. (1990) do not obey surface layer scaling.

The Engineering Science Data Unit (ESDU) wind profile, spectra and coherences (ESDU International 1982; ESDU International 1985; ESDU International 1986) are derived from many sources from all over the world during several decades. ESDU proposes that the turbulence intensities and length scales in the surface layer are dependent on mean wind speed. The argument is that the boundary layer depth increases with increasing wind speed implying larger scales of the turbulence. The other models, relying on surface layer scaling do not contain any information on the boundary layer depth and they contain no explicit reference to the mean wind speed.

The equations of ESDU are, compared to all other spectral models discussed here, by far the most complicated, and will not be cited explicitly. Detailed comparison of these may be found in Mann (1998).

3.2 *Uncertainties in the determination of spectra*

Often spectra are averaged over, say, n consecutive frequencies or wavenumbers to decrease the random error of the estimate. Alternatively, the time series could be divided into n segments of equal duration. Each segment is then Fourier transformed and the spectrum determined as the average of the absolute square of these Fourier transforms. For either definition the statistical uncertainty on spectral density F calculated from a stationary time series is (under the assumption that the time series is long compared to the time scale of the process)

$$\frac{\sigma(F)}{\langle F\rangle} = \frac{1}{n^{\frac{1}{2}}} \tag{16}$$

(Koopmans 1974).

Figure 6 shows the result of an analysis of 14 two-hour time series from the Great Belt. The series have mean speeds U between 16 and 20 m/s and the mean directions are within a narrow range around south where there is an uninterrupted fetch over water for at least 20 km. Also shown in these figures are the ESDU spectra (black lines), the Kaimal spectra (gray curves, eqs. 12 and 13), and the Simiu and Scanlan spectra (gray dashed curves, eqs. 14 and 15). Contrary to the comparison in Figure 5 which had $z = 40$ m and $U = 40$ m/s the model spectra seem to agree fairly well with each other even at low frequencies.

Assuming the stability to be neutral, the variation of spectral densities should obey (16) and the standard deviation at the lowest wavenumbers should be around 25% and 5% at $k_1 = 0.1$ m^{-1}. The observed rms variations are clearly larger, at least 50% at the lowest frequencies (for u and even more for w) and maybe 20% at higher frequencies. Most noticeably, there are spectra with only 10% of the spectral density of the others.

This variation is due to the stability of the atmosphere not being neutral. The case with suppressed

turbulence is slightly stable and has $U = 16$ m/s. From the point of view of aerodynamics this may imply enhanced loads on the bridge deck. While the buffeting load are smaller the loads from vortex shedding can be much larger. Usually vortex shedding from a bridge deck is suppressed or even destroyed by the turbulence in the atmosphere, but if turbulence is absent as in a stably stratified atmosphere (e.g. warm air flowing out over a cold sea) the vortex shedding might be strong.

Unstable stratification also alters the spectrum. Though none of the spectra from the Great Belt are obtained under very unstable situations, an analysis of unstable spectra on the west coast of Norway indicate that the spectra are mainly enhanced (by more than 100%) at *very* low frequencies ($f < 0.02$ Hz). These are not relevant for bridges, but might be for various off-shore production units (Mann 1992).

The effects of stability are expected to disappear at higher wind speeds, but the higher the structure, the more likely stability is playing a role. The 254 m high pylons of the Great Belt East Bridge may therefore experience almost smooth stably stratified flow at 30 m/s or even higher. It is therefore a good idea to continue to carry out wind tunnel tests in both turbulent and smooth flow.

3.3 *Determination of the coherence*

The *coherence* between component i and j of the wind fluctuations measured at two points separated in the horizontal (perpendicular to the mean wind) by Δy and in the vertical by Δz is defined as

$$\mathrm{coh}_{ij}(k_1, \Delta y, \Delta x) = \frac{|\chi_{ij}(k_1, \Delta y, \Delta z)|^2}{F_i(k_1) F_j(k_1)}, \qquad (17)$$

where the cross-spectra, defined as

$$\chi_{ij}(k_1, \Delta y, \Delta z) =$$

$$\frac{1}{2\pi} \int_{-\infty}^{\infty} R_{ij}(x, \Delta y, \Delta z) \mathrm{e}^{-\mathrm{i}k_1 x} \mathrm{d}x \qquad (18)$$

Considerations of coherences (or cross-spectra) are unavoidable in determination of some dynamic loads, f.ex. buffeting on a bridge deck. Often engineers use the so-called square root coherence which is simply the square root of the definition above.

Under the assumption that the segment of the time series is larger than the time scale of the signal the uncertainty of the determination of the coherence is given by

$$\sigma^2(\mathrm{coh}) = \frac{2}{n} \mathrm{coh}(1 - \mathrm{coh})^2 \qquad (19)$$

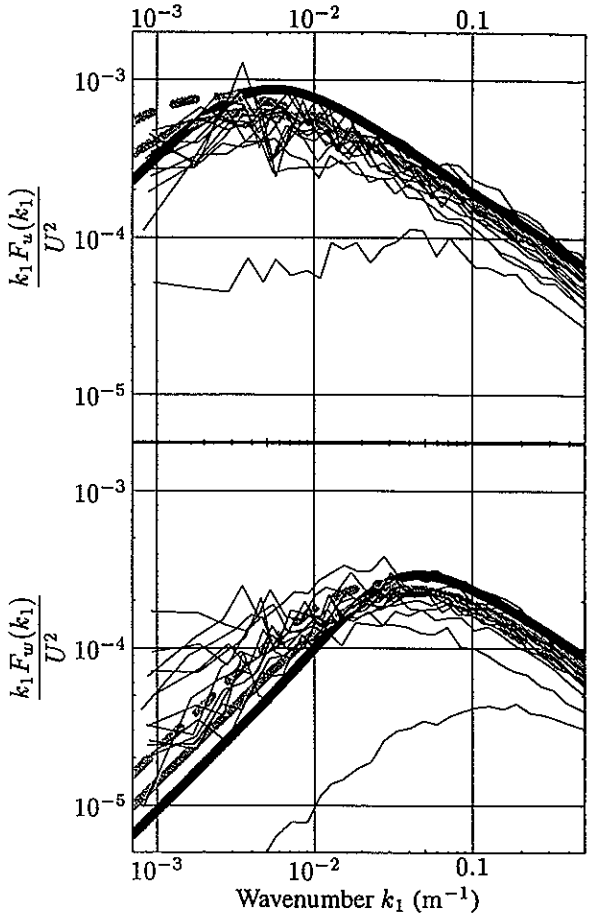

Figure 6: Spectra from the Great Belt Coherence Experiment. Upper plot is u, lower is w. Shown are also three model spectra, the black curve is ESDU, the grey Kaimal, and the grey dashed Simiu & Scanlan

which is valid for large n (Kristensen and Kirkegaard 1986; Mann 1994). For the square root coherence we get

$$\sigma^2(\sqrt{\mathrm{coh}}) = \frac{1}{2n}(1 - \mathrm{coh})^2. \qquad (20)$$

The model coherences given in Simiu and Scanlan (1986) for lateral displacements are

$$\sqrt{\mathrm{coh}_i}(k_1) = \exp(-c\Delta y n), \quad \text{with } n \equiv k_1/2\pi, \qquad (21)$$

with $c = 16$ for $i = u$ and $c = 8$ for $i = w$. This model fit the data quite well at high frequencies, however, these coherences go to one as frequency goes to zero, a property which is in contradiction with observation.

Figure 7 shows coherences calculated from the same data material as for the spectra in Figure 6. The time series were divided into $n = 70$ segments, so $\sigma\sqrt{\mathrm{coh}}$ is 0.08, 0.08 and 0.05 for $\sqrt{\mathrm{coh}}$ =0.1, 0.3 and 0.6. The standard error of the measured coherences is only a bit larger.

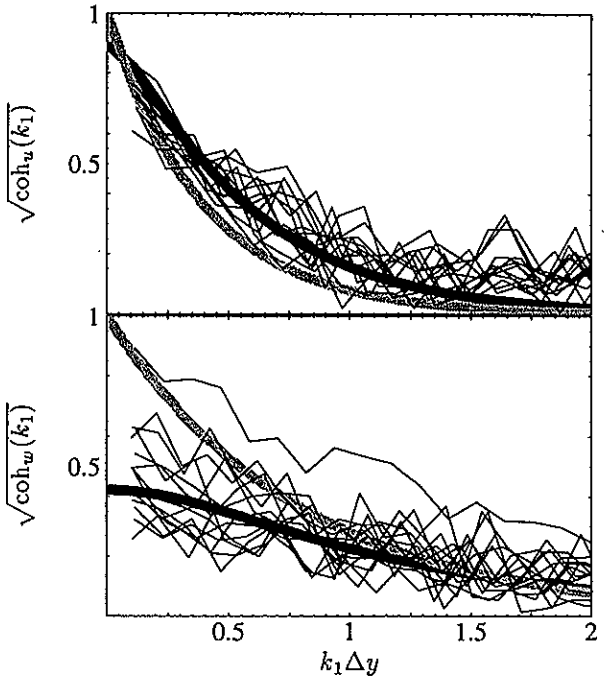

Figure 7: Square root coherences from the Great Belt Coherence Experiment for a lateral displacement of $\Delta y = 32.5$ m. Upper plot is u, lower is w. Shown are model coherence of ESDU (black curve) and of Simiu and Scanlan (eq. 21, gray curves).

3.4 *Modelling and simulation and turbulence*

In an attempt to understand the spectra and coherences measured at the Great Belt, Mann (1994) has constructed a model of the *spectral tensor*:

$$\Phi_{ij}(\boldsymbol{k}) = \frac{1}{(2\pi)^3}\int R_{ij}(\boldsymbol{r})\exp(-\mathrm{i}\boldsymbol{k}\cdot\boldsymbol{r})\mathrm{d}\boldsymbol{r}, \qquad (22)$$

where $\int \mathrm{d}\boldsymbol{r} \equiv \int_{-\infty}^{\infty}\int_{-\infty}^{\infty}\int_{-\infty}^{\infty}\mathrm{d}r_1\mathrm{d}r_2\mathrm{d}r_3$, and Because of homogeneity, the covariance tensor

$$R_{ij}(\boldsymbol{r}) = \langle u_i(\boldsymbol{x})u_j(\boldsymbol{x}+\boldsymbol{r})\rangle \qquad (23)$$

is only a function of the separation vector $\boldsymbol{r}$ ($\langle\ \rangle$ denotes ensemble averaging). The basic idea of the model is the following. Shear has the main responsibility for the anisotropy of turbulence in the lowest part of the atmosphere. Townsend (1976) has shown that assuming the wind profile to be roughly linear it is possible to write a linear differential equation describing the (initial) response of the turbulence to the shear. Mann (1994) used this equation together with consideration on the 'life times' of eddies of different sizes to postulate a crude equilibrium of the shear trying to make turbulence more anisotropic and the decay of eddies, which tends to make turbulence isotropic. Because small eddies decay fast the tensor is isotropic for small scales (k large) while it is anisotropic at larger scales. The model can, on the basis of measured spectra in one point, be used to predict coherences of wind fluctuations measured at two separated point. It models almost any spectral or cross-spectral aspect of the (neutral) turbulence measured at the Great Belt, with only three adjustable parameters.

The spectral tensor is the basis of a Fourier simulation technique (Mann 1998) which produces a three-dimensional field of velocity vectors suitable as input for load calculation on bridges, wind turbines or other structures. It has better than any other model accounted for the complicated spectrum of gustiness as seen from the tip of a rotating wind turbine wing (Petersen et al. 1995). Danish Maritime Institute has done some calculations of the response of a bridge deck using this model.

The model parameters has also been adjusted so that the spectra for u, v, and w fit three widely used spectral models (Kaimal, Wyngaard, Izumi, and Coté 1972; Simiu and Scanlan 1986; ESDU International 1985). In this way the model can be used as input for load calculation for almost any spatially extended structure using as input only the mean wind speed U, the typical height above the terrain z and the surface roughness length z_0.

One major drawback of the model in application to real situations is that it assumes the landscape to be flat and homogeneous. It is well known that the characteristics of turbulence changes at the top of hills, in the wake of hills or close to roughness changes. Currently, we are working on modelling turbulence in complex terrain.

4 CONCLUSION

The basic assumptions of the extreme wind analysis that lead to estimates of the uncertainty of extreme winds seem usually, but not always, as we have seen, to be satisfied.

The estimation of uncertainties on spectra and coherences are much more difficult to quantify. Small changes in the stability of the atmosphere seem to increase the uncertainty even at relatively large wind speeds. The non-uniformity of the surrounding terrain also adds to the uncertainties

Risø is currently working on improving methods to estimate extreme winds anywhere in Denmark and estimate spectra and coherence in complex terrain.

The Danish Energy Agency is acknowledged for support for the preparation of this manuscript through the project WA^{S}P Engineering (EPF-97, 1363/97-0004).

REFERENCES

Abild, J. (1994). *Application of the wind atlas method to extremes of wind climatology.* Technical Report R–722(EN), Risø National Laboratory.

Abild, J., N. G. Mortensen, and L. Landberg (1992). Application of the wind atlas method to extreme wind data. *J. Wind Eng. Ind. Aerodyn. 41–44*, 473–484.

ESDU International (1982). *Charcteristics of wind speed in the lower layers of the atmosphere near the ground: strong winds (neutral atmosphere).* London: ESDU International.

ESDU International (1985). *Charcteristics of atmospheric turbulence near the ground. Part II: single point data for strong winds (neutral atmosphere).* London: ESDU International.

ESDU International (1986). *Charcteristics of atmospheric turbulence near the ground. Part III: variations in space and time for strong winds (neutral atmosphrere).* London: ESDU International.

Gumbel, E. J. (1958). *Statistics of Extremes.* Columbia University Press.

Højstrup, J., S. E. Larsen, and P. H. Madsen (1990). Power spectra of horizontal wind components in the neutral atmospheric boundary layer. In N. O. Jensen, L. Kristensen, and S. E. Larsen (Eds.), *Ninth Symposium on Turbulence and Diffusion*, pp. 305–308. American Meteorological Society.

Jensen, N. O., M. Nielsen, and B. Nielsen (1988). *Climatic overview of the great belt region.* Technical report M–2680, Risø National Laboratory.

Kaimal, J. C. and J. J. Finnigan (1995). *Atmospheric Boundary Layer Flows, Their Structure and Measurement.* New York: Oxford University Press.

Kaimal, J. C., J. C. Wyngaard, Y. Izumi, and O. R. Coté (1972). Spectral charcteristics of surface-layer turbulence. *Q. J. R. Meteorol. Soc. 98*, 563–598.

Klemp, J. V. and D. K. Lilly (1975). The dynamics of wave-induced downslope winds. *JAS 32*, 320–339.

Koopmans, L. H. (1974). *The Spectral Analysis of Time Series.* Academic Press.

Kristensen, L., M. Casanova, M. Courtney, and I. Troen (1991). In search of a gust definition. *Boundary-Layer Meteorol. 55*, 91–107.

Kristensen, L. and P. Kirkegaard (1986). *Sampling problems with spectral coherence.* Technical Report R–548, Risø National Laboratory.

Mann, J. (1992). *Investigation of atmospheric low-frequency turbulence over the ocean.* Technical Report I–634(EN), Risø National Laboratoty.

Mann, J. (1994). The spatial structure of neutral atmospheric surface-layer turbulence. *J. Fluid Mech. 273*, 141–168.

Mann, J. (1998). Wind field simulation. *Probabilistic Engineering Mechanics.* In the press.

Mortensen, N. G., L. Landberg, I. Troen, and E. L. Petersen (1993). *Wind atlas analysis and application program (WASP). Vol 2: User's guide.* Technical Report I–666(EN)(v.2), Risø National Laboratory.

Norwegian Petroleum Directorate (1994). *Regelverksamling for petroleumsvirksamheten (in Norwegian).* Norwegian Petroleum Directorate.

Petersen, E. L. and N. O. Jensen (1995). Storms: statistics, predictability and effects. In A. Horlick-Jones and Casal (Eds.), *Natural Risks and Civil Protection*, pp. 147–177. London: E & FN Spon.

Petersen, J. T., A. Kretz, and J. Mann (1995). Importance of transversal turbulence on lifetime predictions for a hawt. In J. Tsipouridis (Ed.), *5th European Wind Energy Association conference and exhibition. EWEC '94*, Volume 1, pp. 667–673. The European Wind Energy Association.

Simiu, E. and R. H. Scanlan (1986). *Wind Effects on Structures, 2. ed.* John Wiley & Sons.

Townsend, A. A. (1976). *The Structure of Turbulent Shear Flow* (2nd ed.). Cambridge University Press.